JOURNAL OF APPLIED ELECTROCHEMISTRY 22 (1992) 830–834

Current–potential relationships for the half-reactions in two electroless nickel plating baths using the quartz crystal microbalance electrode

A. H. GAFIN, S. W. ORCHARD*

Centre for Applied Chemistry and Chemical Technology, Department of Chemistry, University of the Witwatersrand, Wits 2050, South Africa

Received 28 October 1991; accepted 21 January 1992

Two similar electroless nickel baths, using hypophosphite and dimethylamine borane as respective reducing agents, were investigated using the quartz crystal microbalance electrode. The potential dependences of the half-reactions in the two baths are significantly different, and the nickel plating rates also differ from those observed at the plating potentials in the absence of any reducing agent. In both baths the presence of the anodic half-reaction leads to a substantial increase in the rate of nickel deposition, indicating the existence of important interactions between the half-reactions at the mixed potential.

1. Introduction

In their now classic paper, Wagner and Traud [1] used the concept of the mixed potential to interpret experimental data on the corrosion of the zinc amalgam in acidic solution. At the mixed potential, the two half-reactions involved in the corrosion process (oxidation of Zn to Zn^{2+}, and reduction of H^+ to H_2) occur at equal rates, so that there is no accumulation or loss of electronic charge at the electrode. Through accurate experimentation, they were able to demonstrate that the two half-reactions are mutually independent: that is, the rate of the oxidation half-reaction is independent of the occurrence of the reduction half-reaction, and *vice versa*.

The mixed potential concept is central to the present-day understanding of electrochemical corrosion [2], oxidative leaching of minerals [3], and electroless plating [4]. Generally it appears that, as in Wagner and Traud's study, the rates of the half-reactions involved are effectively independent of each other. However, in recent years, examples of both corrosion [5] and electroless plating [6–11] have been reported in which the half-reactions interact with each other in such a way as to accelerate the overall process. The two half-reactions in electroless plating may be represented in general form as

$$M^{n+}(aq) + ne^- \longrightarrow M(s) \quad (1)$$

$$Red(aq) \longrightarrow Ox(aq) + me^- \quad (2)$$

Interaction between Processes 1 and 2 implies that when both are occurring simultaneously on the surface of M, one or both of their rates are different from their rates measured in isolation at the same potential.

The most direct method of investigating such interactions in electroless plating is to determine the potential dependences of both the anodic and cathodic half-reaction rates in the plating solutions, and then to measure these rates in suitably modified solutions where either the cathodic or the anodic half-reaction can be studied in isolation [8–11]. Such studies have usually involved a working electrode which can serve to monitor both total current and the mass increase associated with the cathodic deposition of metal. We have previously reported a study of a low temperature electroless nickel bath [9] in which the working electrode was a specially designed large surface area, light weight rotating disc electrode (RDE) [12]. The development of the quartz crystal microbalance electrode (QCME) [13, 14] has led to its application in similar studies of both copper and nickel electroless plating baths [8, 10]. The great mass sensitivity of the QCME has the advantage that mass changes on the working electrode can be accurately measured in a few seconds, as compared to times of the order of hours for electrodes where conventional gravimetry is employed.

In the present study, we have used the QCME to study two low-temperature nickel plating baths. These baths, originally reported by Feldstein [15], differ only in respect of the reducing agent employed, which is either sodium hypophosphite or dimethylamine borane (DMAB). The hypophosphite-based bath was previously studied using the RDE [9], where the well-defined hydrodynamic regime at the working electrode surface contrasts sharply with that at the stationary QCME. Furthermore, in the previous study it was shown that the reduction and oxidation half-reactions interacted strongly; the extent of such interaction in the DMAB-based bath was unknown. This paper reports on our findings relating to these issues.

* Author to whom all correspondence should be addressed.

0021-891X/92

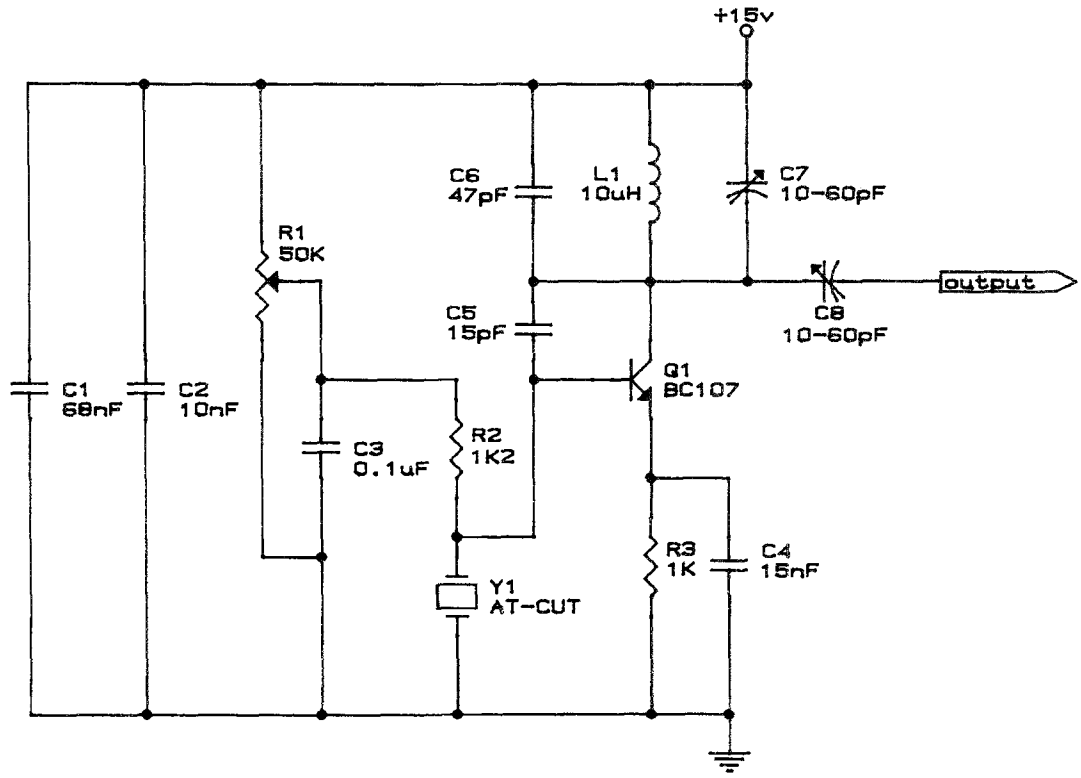

Fig. 1. Oscillator circuit.

2. Experimental details

2.1. *Quartz crystal microbalance electrode*

A planar, 5 MHz, AT-cut quartz crystal disc of diameter 13.7 mm (STC) was used as the oscillating element in a modified Pierce-Miller oscillator circuit (Fig. 1), adapted from that of Weil and coworkers [16]. In our hands, the present, modified circuit was better able to sustain oscillation when the crystal was immersed in solution. Crystal blanks were prepared by evaporating metal on to the two faces in a conventional 'keyhole' pattern. The piezoelectric area was determined by the rear electrode (diam, 5.5 mm) as compared to the 6.6 mm diameter of the front (electrochemical) electrode. The front electrode consisted of successive layers of chromium, palladium and gold, the latter being 80–100 nm thick. The rear electrode was a gold film of about 100 nm thickness. Frequency measurements were made by a Keithley 775A counter-timer controlled by a Philips personal computer (P3105) via an IEEE-GPIB-488 card (National Instruments PC2A).

Of several crystal holders tested in the course of this work, the preferred design is shown in Fig. 2. The body consists of a rectangular Teflon block, 25 mm × 25 mm × 30 mm. Silver epoxy was used to connect the leads (~ 40 cm long, mostly coaxial) from the oscillator circuitry to the quartz crystal faces.

2.2. *Electrochemistry*

The front face coating (exposed area 0.404 cm^2) of the quartz crystal served as the working electrode (WE) in a three-electrode system. The counter electrode was a nickel flag (10 mm × 15 mm) parallel to and facing the quartz disc WE. A saturated calomel electrode (SCE), to which all quoted potentials are referred, was used as the reference electrode in a Luggin probe containing 1 M KCl and positioned about 5 mm from the WE. Electrochemical control was by a potentiostat with a grounded WE designed locally at MINTEK. The potentiostat was linked to the PC by a 12

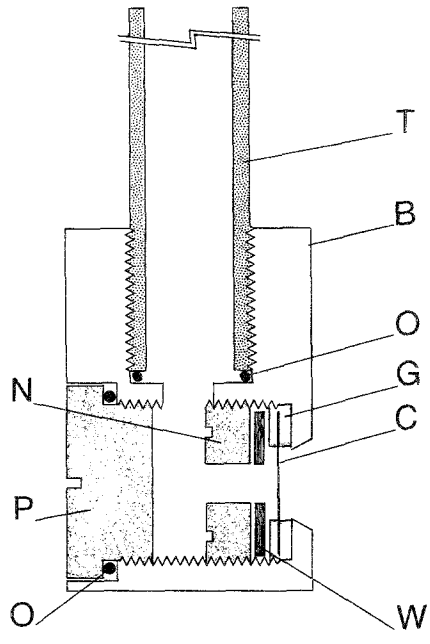

Fig. 2. Holder for quartz crystal oscillator. (T – Pyrex tube; B – Teflon body; O – O-ring; G – silicone gasket; C – quartz crystal; W – washer; N – Perspex nut; P – Teflon plug).

Table 1. Compositions of the two electroless nickel plating baths

Reagent	*Bath 1* M	*Bath 2* M
$Ni_2SO_4 \cdot 6H_2O$	0.095	0.095
$Na_4P_2O_7 \cdot 10H_2O$	0.110	0.110
NH_3 (pH 10.8)	~0.34	~0.34
$NaH_2PO_2 \cdot H_2O$	0.280	–
$(CH_3)_2NH \cdot BH_3$	–	0.051
KCl	1.00	1.00

bit AD–DA interface card (IBM DACA) which permitted software monitoring of current. The electrochemical cell (METROHM) was water-jacketed and of 100 cm^3 volume. A water circulator/regulator (MGW–LAUDA) allowed temperature control to better than 0.1° C. Constant, moderate stirring via a magnetic stirrer was used throughout all experiments; no attempt was made to exclude air from the solutions.

2.3. *Plating bath formulations*

The compositions of the two plating baths studied are given in Table 1. They are almost identical to those proposed by Feldstein [15], except for the addition of KCl which serves here as a supporting electrolyte, reduces any uncompensated solution resistance, and has been shown to have a minimal effect on the plating rate of the hypophosphite-based bath [6]. Solution volumes of 100 cm^3 were freshly prepared for all experiments from AR-grade reagents where available, and water from a Millipore Milli-Q unit.

2.4. *Procedure*

Electroless plating was initiated on the WE by polarizing it to −1.00 V/SCE for 10–15 s. A subsequent open circuit potential of about −0.94 V (hypophosphite bath) or −1.02 V (DMAB bath) was evidence of successful initiation. The potential of the WE was then stepped to the required initial value in the range −0.50 to −1.25 V. Once the electrode had stabilized, usually within about 15 s, current and oscillator frequency were logged for 60–100 s. The average current was used to calculate the nett current density j; the cathodic deposition partial current density j_c was calculated from the mass of electroless nickel deposited which, in turn, was obtained from the Sauerbrey equation [13, 14, 17]. Allowance was made for the small amounts of phosphorus or boron in the deposits [9, 15]. The anodic partial current density j_a was calculated as $j - j_c$, where j_c is considered to be negative when plating is occurring. From a series of measurements at different potentials, plots of j, j_c and j_a against E were constructed.

To avoid excessive build up of electroless nickel on the WE, it was periodically stripped in a room temperature solution of Na_2SO_4 (0.1 M) and H_2SO_4 (0.2 M), using a slow sweep from −0.20 to +0.10 V/SCE, and then holding at the final potential until all the deposit was removed.

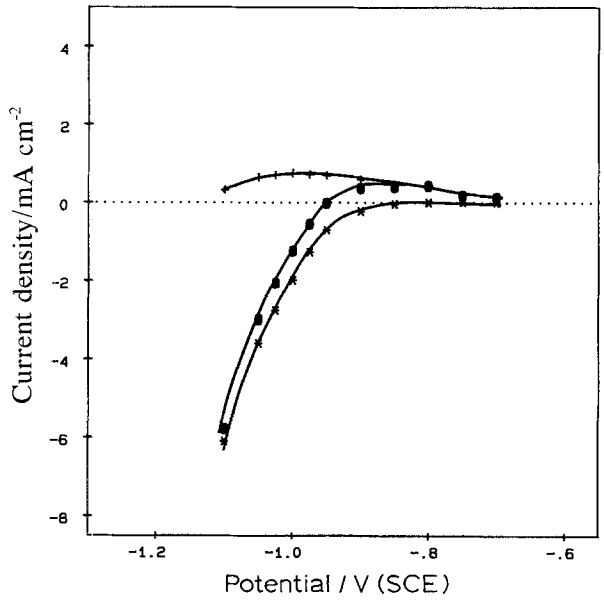

Fig. 3. Plots of net current density, j (●), and cathodic and anodic partial current densities, j_c (*) and j_a (+) against potential for the hypophosphite bath (bath 1) at 20° C.

3. Results and discussion

Figures 3 and 4 show plots of j, j_c and j_a against E, obtained for the two electroless baths at 20° C. While there are some general similarities between the figures, there are important detailed differences. In the hypophosphite bath, j_a shows little dependence on potential around the plating potential, and the overall rate is under anodic control. The DMAB bath exhibits joint anodic–cathodic control of the rate. The maximum rate of DMAB oxidation occurs at about −0.85 V, and is over three times the maximum rate for hypophosphite oxidation. However the high maximum in j_a for DMAB is not reflected in the plating rate, since it occurs in a region where nickel is scarcely depositing at all.

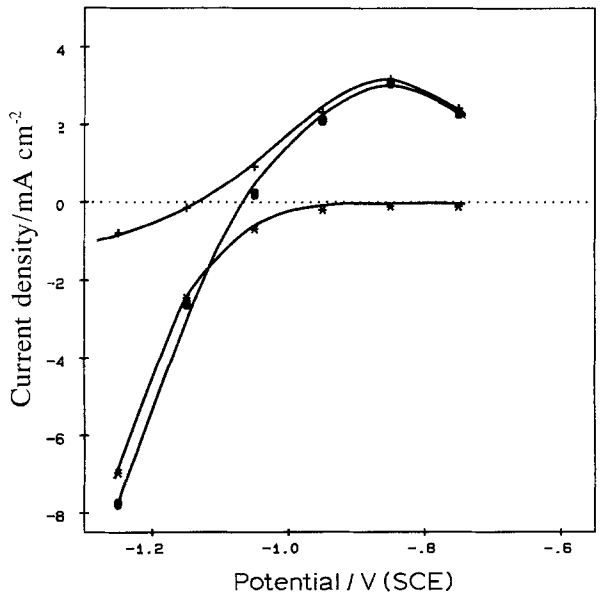

Fig. 4. Plots of net current density, j (●), and cathodic and anodic partial current densities, j_c (*) and j_a (+) against potential for the DMAB bath (bath 2) at 20° C.

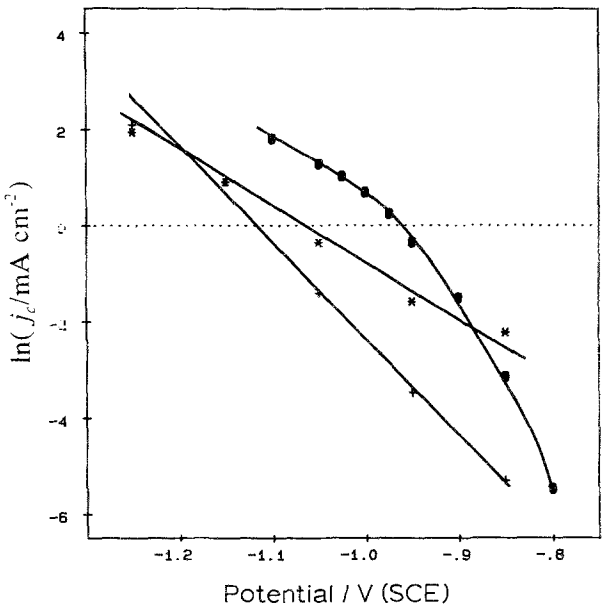

Fig. 5. Plots of ln j_c against E for data from Figs 3 and 4, as well as for a solution containing no reducing agent. All data obtained at 20°C. (●) $H_2PO_2^-$ bath, (*) DMAB bath, (+) no reducing agent.

In Fig. 5, the j_c data of Figs 3 and 4 are plotted in semilog form. Also shown are points obtained from microbalance measurements in a bath free of both reductants, but otherwise identical to those of Table 1. Over most of the relevant potential range, the rate of nickel deposition is substantially higher in the presence of hypophosphite than it is with either DMAB or no reductant at all. At −0.95 V, for example, the relative cathodic rates (hypophosphite : DMAB : no reductant) are in the approximate ratio 22 : 7 : 1. This clear indication of substantial mechanistic differences between the systems is further emphasized by the differing slopes and curvature of the three plots. In the case of the hypophosphite bath particularly, it appears that while the reductant is being oxidized, the reduction of nickel ions is substantially accelerated. Clearly, the two half-reactions are not occurring independently, and the anodic process is in some way influencing the rate of the cathodic process.

Several possible modes of interaction between the two half-reactions may be considered. Firstly, there could be a direct electron transfer process from $H_2PO_2^-$ to Ni^{2+} on the electrode surface. There are precedents for such direct (or chemical, as opposed to electrochemical) mechanisms of surface redox reactions in corrosion-related processes [18]. However, in the present case there is no evidence in the individual current-potential curves of any such coupling between the anodic and cathodic rates, and this mechanism can be safely discarded. One is left with the possibility that either hypophosphite, or an intermediate or product derived from this reagent, is responsible for accelerating the rate of Ni^{2+} reduction. U.v.-visible spectrophotometry does not reveal any signs of complexation between Ni^{2+} species in the bulk solution and $H_2PO_2^-$, at the concentrations used in the plating solution [15, 19]. This does not rule out the possibility of a surface interaction between the two, and here the tautomeric form of $H_2PO_2^-$, involving 3-valent phosphorus, should be considered.

Scheme 1: Tautomeric forms of $H_2PO_2^-$

The 3-valent form has been implicated as the readily oxidizable tautomer [20], and could be capable of acting as a bridging ligand between the Ni surface and Ni^{2+} in solution, thus stabilizing the latter at a close enough distance for electron transfer to occur more readily:

Scheme 2: $H_2PO_2^-$ as a bridging ligand

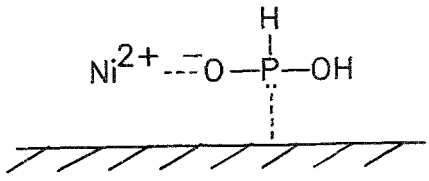

(In support of the above scheme, it should be noted that certain additives, present in trace amounts, are capable of both stabilizing and accelerating electroless copper baths [21–23], and surface adsorption appears to be critical to their mode of action. Schoenberg [21] has in fact proposed that 7-iodo-8-hydroxyquinoline-sulphonic acid accelerates electroless copper plating through a similar bridging mechanism. Wiese and Weil [8] have also postulated the need for chemisorbed catalysts in order for electroless copper plating to proceed.)

Other possible modes of interaction between the two half-reactions are via either the phosphite (HPO_3^{2-}) product of $H_2PO_2^-$ oxidation, or the small amount (~4% [9]) of phosphorus which is incorporated in the surface deposit. $H_2PO_3^-$ is a moderately good ligand for Ni^{2+}, and almost certainly better than $H_2PO_2^-$ [24], but we have been unable to locate stability constant data for Ni^{2+} with HPO_3^{2-}, which will exist in preference to $H_2PO_3^-$ at the high pH of the present study. We have observed only minimal differences between the uv-visible absorption spectra of the normal plating bath, and a solution in which the $H_2PO_2^-$ was replaced by HPO_3^{2-}; thus there is no clear evidence for substantial interaction between Ni^{2+} and HPO_3^{2-} in bulk solution.

An interaction between the half-reactions also occurs in the DMAB bath; this is particularly evident at the more positive potentials of those plotted in Fig. 5. However, the experimental evidence available at present does not appear to be sufficient for any confident predictions to be made as to the details of the

interactions, for either the hypophosphite or the DMAB baths.

Plots of j, j_c and j_a against E obtained with the hypophosphite bath at a higher temperature (35 °C) are fully consistent with the 20 °C data of Fig. 3. The plating rate shows a significant increase with temperature, but remains under anodic control. Between -0.9 and -1.1 V, the rate of the anodic half-reaction is essentially constant. These temperature and potential effects and the insensitivity of the rate to agitation [12, 25], are best explained by a mechanism in which surface rearrangement of $H_2PO_2^-$ from the 5-valent phosphorus form to the 3-valent form, is rate-determining.

4. Conclusions

The two electroless plating baths studied are identical in composition, except for the reductant, and operate under similar conditions of temperature and pH. By resolving the individual half-reactions, and their potential dependence, we have shown that there are important differences between the baths as regards the anodic and cathodic processes, and the overall rate control. Both baths exhibit significant interactions between the half-reactions, but the mechanism of interaction remains to be determined.

Acknowledgements

We thank Professor R. D. Hancock for valuable discussions: University electronics technicians, especially Mr S. Fripp for advice and assistance; and also we thank the University of the Witwatersrand and the Foundation for Research Development for financial support.

References

[1] C. Wagner and W. Traud, *Z. Elektrochem.* **44** (1938) 391.
[2] J. O'M. Bockris and A. K. N. Reddy, 'Modern Electrochemistry', Vol. 2, Plenum Press, New York (1970).
[3] M. E. Wadsworth, in 'Electrochemistry and Solid State Science Education at the Graduate and Undergraduate Level', (edited by W. H. Smyrl and F. McLarnon), Electrochemical Society Proceedings, Volume 87-3, Pennington, NJ (1987) pp. 220–32.
[4] M. Paunovic, *Plating* **51** (1968) 1161.
[5] T. N. Andersen, M. H. Ghandehari and H. Eyring, *J. Electrochem. Soc.* **122** (1975) 1580.
[6] F. M. Donahue, *ibid.* **119** (1972) 72.
[7] A. Vashkyalis and Y. Yachgauskene, *Elektrokhimiya* **17** (1981) 1515.
[8] H. Wiese and G. Weil, *Ber. Bunsenges. Phys. Chem.* **91** (1987) 619.
[9] S. W. Orchard, *Plating* **75** (1988) 56.
[10] B. J. Feldman and O. R. Melroy, *J. Electrochem. Soc.* **136** (1989) 640.
[11] P. Bindra and J. Roldan, *J. Appl. Electrochem.* **17** (1987) 1254.
[12] S. W. Orchard, *ibid.* **18** (1988) 666.
[13] M. R. Deakin and D. A. Buttry, *Anal. Chem.* **61** (1989) 1147A.
[14] R. Schumacher, *Angewandte Chemie* **29** (1990) 329.
[15] N. Feldstein, *RCA Review* **31** (1970) 317.
[16] M. Benje, M. Eiermann, U. Pittermann and K. G. Weil, *Ber. Bunsenges, Phys. Chem.* **90** (1986) 435.
[17] G. Z. Sauerbrey, *Z. Phys.* **155** (1959) 206.
[18] F. Mansfeld and V. Kenkel, *Corros. Sci.* **16** (1976) 653.
[19] A. H. Gafin and S. W. Orchard, unpublished data.
[20] A. Hickling and D. Johnson, *J. Electroanal. Chem.* **13** (1967) 100.
[21] L. N. Schoenberg, *J. Electrochem. Soc.* **119** (1972) 1491.
[22] M. Hannemann and M. Siegel, *Feingeraetetechnik* **31** (1982) 30; *C.A.* **96**: 203830a (1982).
[23] M. Paunovic and R. Arndt. *J. Electrochem. Soc.* **130** (1983) 794.
[24] R. M. Smith and A. E. Martell, 'Critical Stability Constants', Vol. 4, Plenum Press, New York (1976).
[25] N. Feldstein and P. R. Amodio, *Plating* **56** (1969) 1246.